MASTER COPY KEEP THIS COPY FOR REPRODUCTION PURPOSES

(2)

AD-A254 831

ION PAGE

Form Approved
OMB No. 0704-0188

1. A	July 27, 1992	3. REPORT TYPE AND DATES COVERED Final Report: 10/1/88 - 3/31/92

4. TITLE AND SUBTITLE
Massively Parallel Optical-to-Electronic Data Transfer

5. FUNDING NUMBERS
DAAL03-88-K-0175

6. AUTHOR(S)
C. M. Verber, J. P. Uyemura, and U.-S. Rhee

7. PERFORMING ORGANIZATION NAME(S) AND ADDRESS(ES)
School of Electrical Engineering, Georgia Tech,
777 Atlantic Dr., NW, Atlanta, GA 30332-0250
and
Center for Applied Optics, University of Alabama at Huntsville, Huntsville, AL 35899

8. PERFORMING ORGANIZATION REPORT NUMBER
E-21-651 Final Report

9. SPONSORING/MONITORING AGENCY NAME(S) AND ADDRESS(ES)
U. S. Army Research Office
P. O. Box 12211
Research Triangle Park, NC 27709-2211

10. SPONSORING/MONITORING AGENCY REPORT NUMBER

11. SUPPLEMENTARY NOTES
The view, opinions and/or findings contained in this report are those of the author(s) and should not be construed as an official Department of the Army position, policy, or decision, unless so designated by other documentation.

12a. DISTRIBUTION/AVAILABILITY STATEMENT
Approved for public release; distribution unlimited.

12b. DISTRIBUTION CODE

13. ABSTRACT *(Maximum 200 words)*

The design and experimental verification of a system composed of a page-oriented holographic binary memory and a compatible CMOS chip for receiving the stored data are presented. The optical retrieval system is novel in that the Bragg cell for selecting positions in the memory plane is coupled to the angle-selecting Bragg cell by an optical fiber array. This relieves several optical constraints and allows compact packaging of the system. The design, analysis, and fabrication of the electronic RAM array was performed using the 2-micron CMOS process available through MOSIS. A high-speed integrated CMOS process was chosen for its logic-integration capabilities. Adding the photodetector and associated circuitry to the normal design procedures provides for direct optical-to-electronic interfacing. Based on the measured efficiency of the optical system and the measured sensitivity of the CMOS detectors, it is predicted that a memory with a page size of 128 x 128 bits and a read rate of 5×10^5 pages per second could be constructed. A variety of applications beyond ROM-to-RAM data transfer are discussed.

14. SUBJECT TERMS
Holography, Optical Data Storage, Opto-electronic CMOS, Photopolymers

15. NUMBER OF PAGES
34

16. PRICE CODE

17. SECURITY CLASSIFICATION OF REPORT	18. SECURITY CLASSIFICATION OF THIS PAGE	19. SECURITY CLASSIFICATION OF ABSTRACT	20. LIMITATION OF ABSTRACT
UNCLASSIFIED	UNCLASSIFIED	UNCLASSIFIED	UL

MASSIVELY PARALLEL OPTICAL-TO-ELECTRONIC DATA TRANSFER

FINAL REPORT

C. M. VERBER, J. P. UYEMURA, AND U.-S. RHEE

JULY 27, 1992

U.S. ARMY RESEARCH OFFICE

CONTRACT NUMBER DAAL03-88-K-0175

GEORGIA INSTITUTE OF TECHNOLOGY
AND
UNIVERSITY OF ALABAMA AT HUNTSVILLE

TABLE OF CONTENTS

LIST OF APPENDICES

LIST OF FIGURES

LIST OF TABLES

1. INTRODUCTION

1.1 Motivation

This program was motivated by a series of discussions and comments at a DoD-sponsored Workshop on Artificial Intelligence, Gold Lake, Colorado, 1987 in which it was pointed out that one of the bottlenecks in data-intensive computing, such as that required for the implementation of artificial intelligence machines, is the rate at which data stored in a large-capacity read-only memory (ROM) can be transferred to the random-access memory (RAM) which is accessed during the computing process.

In discussions at the Gold Lake meeting, it was concluded that developments in holographic recording materials[1] and optical components since the early work on page-oriented holographic memories[2] in the 1970's made it worth reinvestigating the possibility of a system in which it many pages of binary data could be stored, each page containing up to 10^5 bits, in a 1 mm^3 segment of an extended storage plane. To allow all of the holograms to be reconstructed in the same image plane, Fourier-transform holograms would be used, and the image plane would be in the back focal plane of a complimentary Fourier-transform lens as shown in Figure 1.1. To further increase the capacity of the memory, either angle- or wavelength- multiplexing would be used, with a consequent requirement of a thick holographic material.

Even though it was possible to conceive of hardware approaches for a POHM retrieval system which would make it possible to access a page and transfer the data to a detector array in several microseconds, it was recognized that, even if the potential of the POHM could be realized, there was no extraordinary system gain to be anticipated if the data were, for example, transferred to a CCD array which would then allow only serial access to the data. As a consequence, it was decided that, as a companion to the holographic ROM is would be necessary to develop a detector array which, at the lowest level, would be a RAM chip with a holographically-addressed photodetector in each cell and which, at a higher level, would contain special-purpose processing electronics tailored to a specific task; an optoelectronic integrated VLSI circuit.

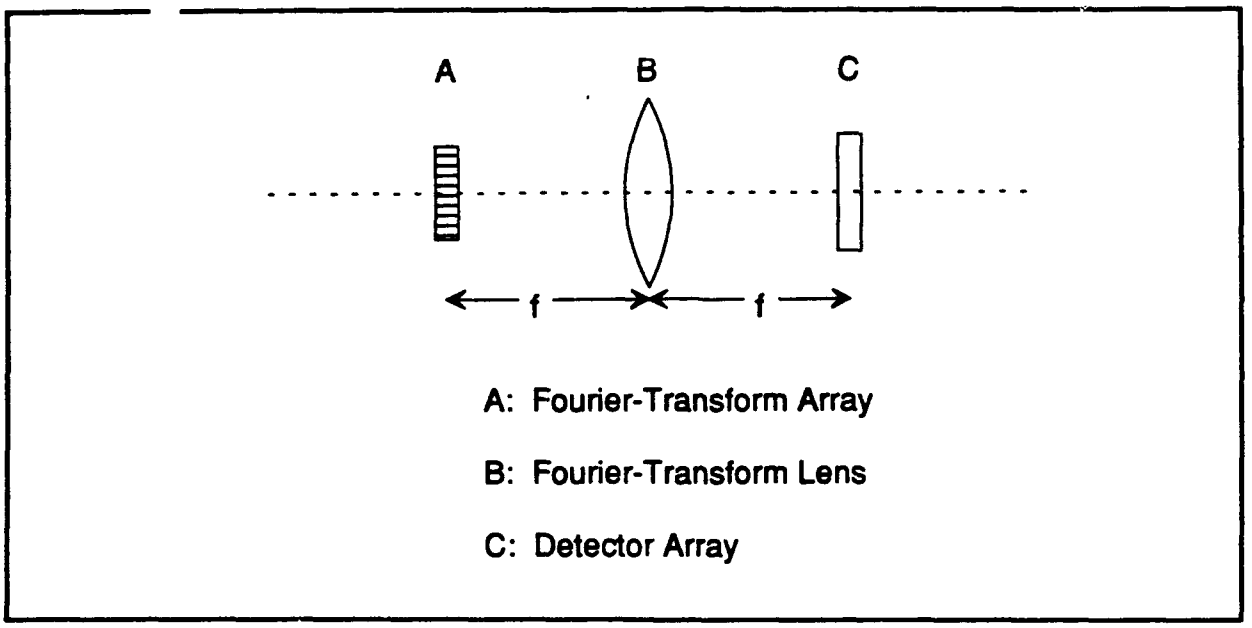

Figure 1.1 Basic geometry of output portion of the page-oriented holographic memory. The Fourier-transform lens ensures that the output of each of the Fourier-transform holograms registers properly on the detector array.

A natural characteristic of the page-oriented memory is the pre-organization of data into blocks, a characteristic which is compatible with the AI or expert system application. During the effort to design and build a prototype POHM, it became evident that there are many other POHM applications, some of which may be significantly more interesting than A machines. These are discussed in Section 7 of this report.

We review here the accomplishments of the program. Many of the details are contained in the two Ph.D. thesis and seven manuscripts which resulted from this work and are appended to the report. Those areas not covered in the appendices are treated more thoroughly here.

1.2 Historical Background

Smits and Gallagher[3] first discussed the Page Oriented Holographic Memory (POHM) in 1969. Despite massive efforts to commercialize this concept in the late 1960s and early 1970s, no product arose. The reasons for this "failure" appear to have been both conceptual and technological. One conceptual failure was the insistence that the POHM exhibit read/write capability. We now know this will be difficult at best but that there are many applications, including data-base and knowledge-base machines, which have a great need for

read only memories with high storage capacity and high random-access speed. A second conceptual failure was the demand for electronic readout. The POHM could produce, perhaps, 10^5 bits each microsecond in a parallel 2-D page. To handle this electronically involves either of two major difficulties, 10^5 parallel detectors and subsequent parallel electronics or full or partial serialization of the page with the consequent major slowdown in speed and a consequent reduction in the advantage over conventional memories.

One of the most through treatments of the problem of "Data Storage in Volume Holograms" is to be found in the 1974 thesis by Richard Zech[4]. A review of holographic storage of digital data[5] appears in *Handbook of Optical Holography.*

Page-oriented holographic memories were abandoned in the late 1970's for a variety of reasons. a) The emphasis was on erasable memory systems which resulted in very severe memory-material requirements. b) The POHM output interfaced with an electronic RAM from which the data then had to be retrieved serially. This negated the speed advantage which derives from the parallel transfer of a full page of data. c) The readout system was large and rather clumsy which made interfacing with digital systems in a working environment rather difficult.

1.3 Program goal

The goals of this program were to design a compact, high-capacity POHM system which would overcome the difficulties listed above, to develop a design methodology for the optimization of the POHM system and to design and demonstrate a limited-capacity system which would validate the design.

2. SYSTEM OVERVIEW

The holographic ROM is organized in a hierarchy of pages with N_1 bits per page, hologram locations with N_2 holograms per location, and a memory plane with N_3 hologram locations. The overall design goals are to maximize the capacity of the memory, which is given by

$$N = N_1 N_2 N_3 \tag{1}$$

while maintaining rapid page-access time and reasonable read-system size. The access-time goal is to be able to access a page in times on the order of microseconds. It is desired that the read system fit in a standard 19" rack for compatibility with electronic computing equipment. Since the writing process is performed off-line, there are no speed or size requirements for the write system. Therefore the major optical problem is the design of the read system. This is described below.

2.1 Wavelength- Versus Angle-Multiplexing

The first major overall system design choice was that of using wavelength or angle multiplexing to superimpose the holograms in each of the recording areas. The choice of angle multiplexing was made on the basis of existing hardware according to the following arguments.

For a symmetric hologram of thickness d and grating wavelength Λ, the angular range between the peak and the first minimum of the diffraction efficiency versus angle curve is approximately

$$\Delta\Theta \approx \frac{d}{\Lambda} \tag{2}$$

which for an optical wavelength of 0.5145 μm, a 1-mm-thick recording material, and a Bragg angle of 20 degrees, is an angle of 0.43 degrees (0.75 mrad). A TeO_2 Bragg cell with an acoustic velocity of 6.16×10^4 cm/sec and a center frequency of 60 Mhz has an angular

deflection range of 33 mrad. Therefore, if the angular separation between the pages is $2\Delta\Theta$, 22 individual data pages can be addressed in a single recording volume.

The corresponding equation for wavelength resolution is

$$\Delta\lambda = \frac{\lambda^2}{2d}\frac{\cos\Theta_B}{\sin^2\Theta_B} \tag{3}$$

which under the same conditions yields a wavelength of 2.1 nm between the peak and the first minimum of the wavelength-tuning curve. To get the same storage capacity as in the angle-multiplexing case, as tuning range of 92 nm is required. Although, in principle, the wavelength-multiplexed approach would lead to a simpler optical system, than the angle-multiplexed approach, there are no compact, rapidly tunable lasers available, especially in the visible region of the spectrum. It might be possible to build a dye laser with a tunable rear reflector composed of a Bragg cell used in retroreflection, but such an undertaking was beyond the scope of this program. Another, less versatile approach to the construction of a source for wavelength multiplexing is to use an assembly of laser diodes of different wavelengths. This, coupled with the position-addressing scheme described below, might be a good solution to the source problem, but the requisite lasers were not available for this program.

The angle multiplexing problem can be solved by taking advantage of recent advances in laser diode arrays which allows the use of a separate laser[6] to address each angle-multiplexed hologram in given volume. However, this method would seem to be limited to a few angles, while, as shown above, angle multiplexing can, in principle allow up to 22 addressable pages in a 1-mm-thick recording material. A Bragg-cell approach to angle multiplexing was therefore selected.

2.2 Architecture of the Holographic-ROM-to-CMOS Data-Transfer System

The major constraint under which the POHM was designed was that, in order to prevent alignment and access-time problems, the system would have no moving parts. To accomplish the reconstruction of each member of an array of holograms with proper bit registration on the same detector array without moving each hologram into position before readout, requires that the holograms be located in the front focal plane of a Fourier-transform

lens. This, in turn, requires that the holograms themselves be records of the Fourier-transforms of the data mask so that the retransform operation results in an image of the data pattern. As shown in Figure 1.1, this sets the basic geometry of the output half of the read system, a 2-f arrangement with the hologram array at the front focal plane and the detector array at the rear focal plane of a Fourier-transform lens.

Addressing the memory requires both position and angle deflection of the read beam. Although electrooptic schemes were considered, it was decided that they could not compete with the versatility and performance of acoustooptic methods, even though, as will be see, the characteristics of available Bragg cells are a major factor in limiting the performance of the POHM.

The first set of designs to be studied were based on the use of two Bragg cells, one to select the position on the memory plane, the other, set close to the memory plane, to select the angle. Even the best of these designs suffer from the disadvantages of large size, critical alignment requirements which necessitate support on optical tables, and an unavoidable restrictions on the system capacity which results from the fact that free-space optics and large optical paths are required.

Figure 2.1 shows the solution to these problems on which the current design is based. A array of optical fibers is used to decouple the position-selection and angle-selection functions. The advantages are:

- Physical separation of the two Bragg cells which allows the entire POHM to be mounted in two 19" racks connected by a fiber cable.
- Increased memory capacity since many optical constraints are relieved.
- Design versatility since the same laser can be used to address several memory planes or a 1-D Bragg cell can be used to address a 2-D memory plane simply by properly arranging the output ends of the fibers.

The details of the fiber addressing system including loss measurements and displays of data reconstructed from angle-multiplexed holograms are discussed in Section 3. The characteristics of the CMOS electrooptic VLSI circuit are discussed in Section 4.

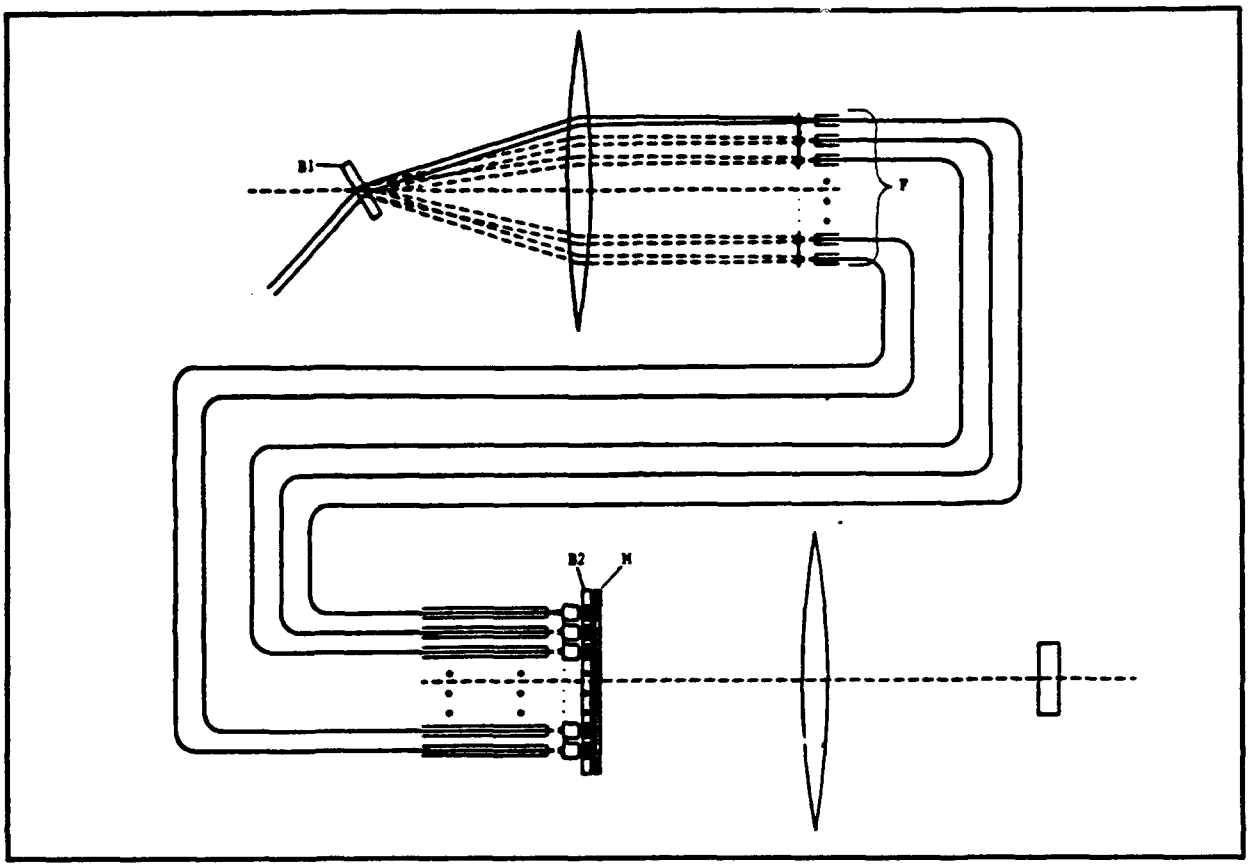

Figure 2.1 Fiber-based address system in which the position-addressing Bragg cell, B2 and the angle-addressing Bragg cell array B2 are optically coupled by a Fiber Array F. B2 is in close proximity to the holographic memory plane M.

2.3 Estimate of System Capacity

An initial estimate of the system capacity can be performed simply on the basis of independent estimates of N_1, N_2, and N_3, although as will be seen, this gives a somewhat optimistic result. N_1 is limited by the capability of the CMOS process to about 10^3 for a single chip and to about 10^6 for wafer-scale integration. On the basis of a 1-mm-thick recording material, values of N_2 of up to 50 can be achieved with either angle- or wavelength-multiplexing. Initial estimates of a 100 × 100 hologram array lead to a value of N_3 of 10^4, or a value of N between 5×10^9 and 5×10^{11}.

One of the initial accomplishments of the program was to develop a design methodology which considered the interaction between the various system components in a way which both allowed design optimization and provided a more realistic method of calculating the system capacity. This method, which is described in Appendix A, predicts a

maximum capacity of 2×10^9 bits for the holographic memory system under the constraint that there are no mechanically moving parts.

3. THE READ SYSTEM

3.1 Hologram Size

The goal of the POHM design studies was to maximize the data-storage capacity of the system without sacrificing other system performance parameters such as retrieval time and fidelity of the reconstructed data page. The effect of hologram size was modeled by considering the effects of apertures in the Fourier-transform plane of a 4-f imaging system. Both a computationally-intensive convolution method, and a faster but less satisfactory FFT model were used. These, and corresponding laboratory results are discussed in Appendix A and in Appendix B, a manuscript submitted to Applied Optics.

In both the computational and the laboratory studies, the data page was represented by an array of 30 × 30 μm square "bits" on 100 μm centers. In the most severe test of crosstalk, the center bit was a zero (opaque) while all the rest were ones (transparent). The hologram area was modeled either as a hard aperture or as a Gaussian aperture, the later case more closely resembling that of the hologram extent being determined by the Gaussian reference beam or the read beam in the actual POHM system.

The aperture acts as a low-pass filter in the Fourier-transform plane, truncating the data page's spatial frequency spectrum. The consequent distortion in the retransformed image results in bit-spreading cross talk and in a reduction in "impact efficiency", that is the fraction of the light which should have landed on a detector which actually got there. Representative results are shown in Figure 3.1. Comparing curves a) and c) we see that for a 30 μm detector, we loose about 15% in impact efficiency in going from a 3-mm-diameter to a 1-mm-diameter Gaussian aperture. Under the same conditions, as seen from curves d) and e), the crosstalk goes from -15 dB to essentially zero.

3.2 Experimental Results

Several distinct geometries were considered and tested for use in the prototype system. The preferred system is shown in Figure 3.2. The volume selection components consisting of the 1st Bragg cell, a focusing lens, a micro-lens array, an optical fiber bundle, and a collimating grin lens output array. The read system in Figure 3.2 is preferred due to it's compactness although, if necessary, two additional lenses inserted between the Bragg cell

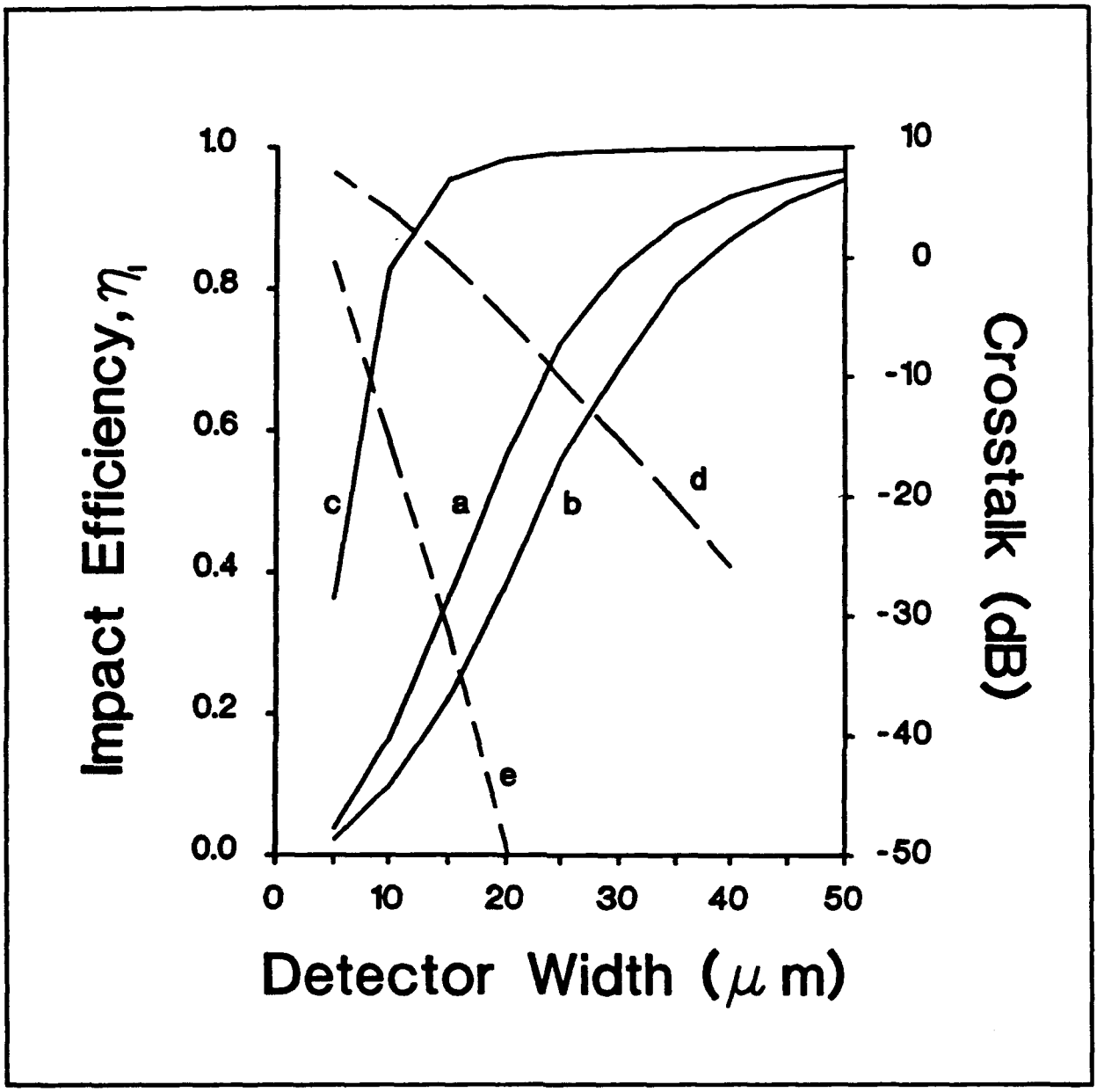

Figure 3.1 The impact efficiency (solid lines) for different aperture diameters is plotted for a) d = 1 mm and a Gaussian aperture, b) d = 1 mm and a circular aperture, and c) d = 3 mm and a Gaussian aperture. Also, the crosstalk (dashed lines) is plotted for d) d = 1 mm and e) d = 3 mm with a Gaussian aperture and $\gamma = 2$. In all of these curves, f = 100 mm and $\lambda = 0.5145$ μm.

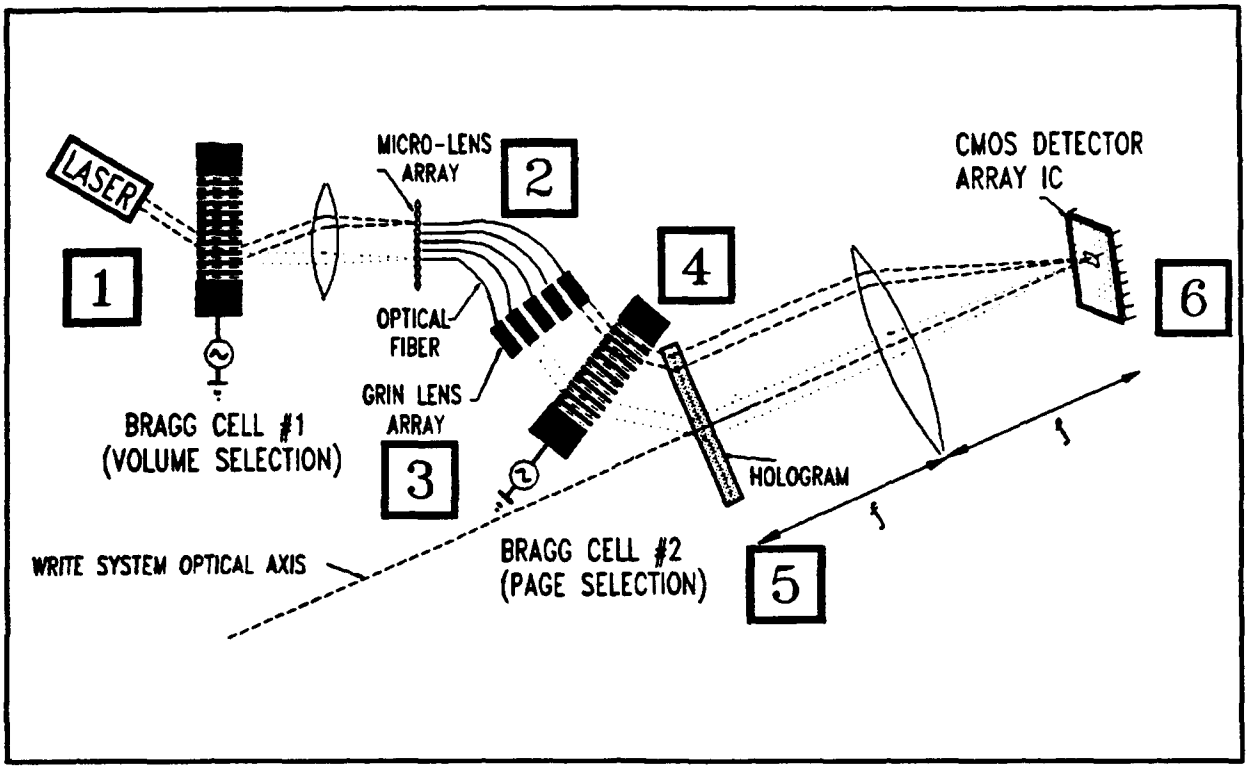

Figure 3.2 The read system. The components are described in Table 3.1.

and the hologram can be used to provide an trade off between angle and beam size at the hologram plane. The write system shown in Figure 3.3 was used because of its simplicity and its compatibility with the read geometry. Keys to the components of the read-system (Figure 3.2) and the write system (Figure 3.3) follow.

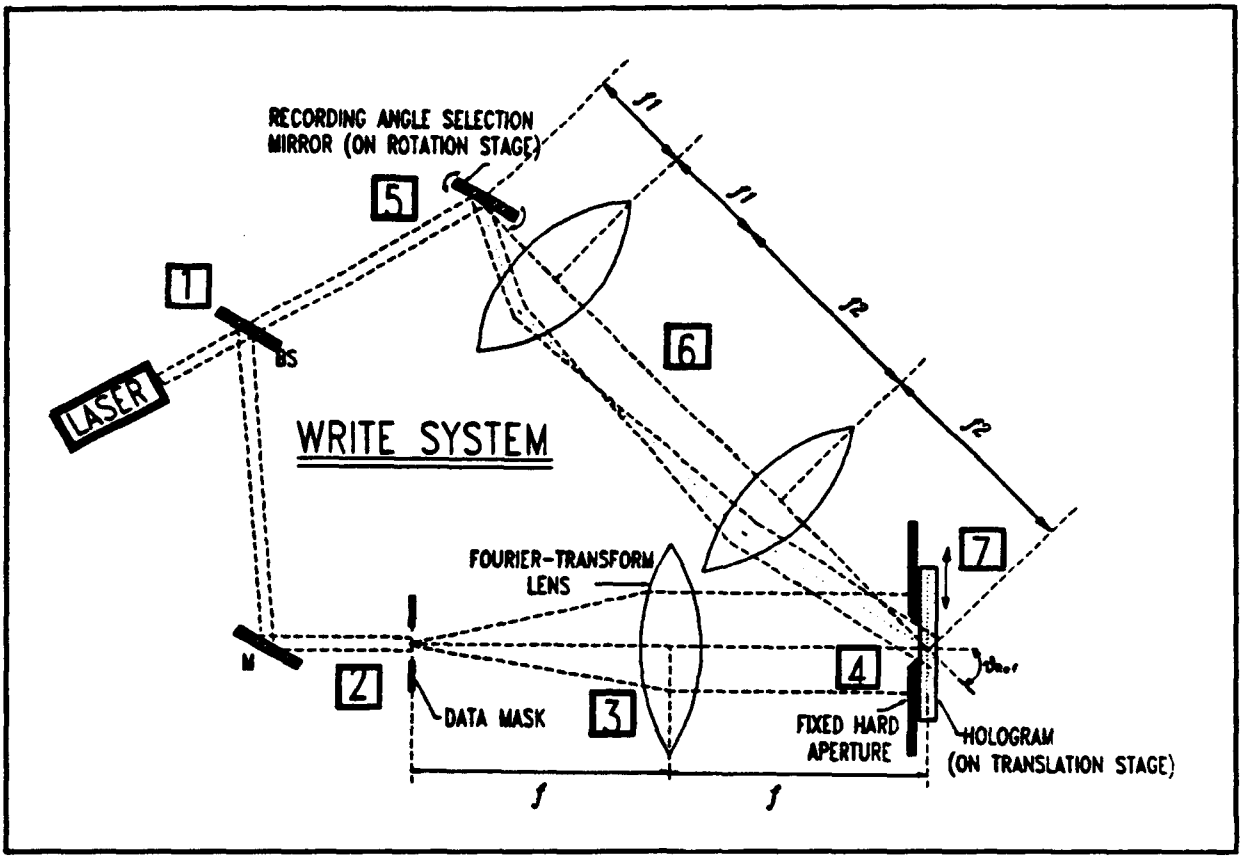

Figure 3.3 The write system. The components are described in Table 3.2.

TABLE 3.1 READ SYSTEM COMPONENTS

1 Collimated output from an argon laser is directed to the desired location on the hologram substrate via deflection from the first Bragg cell.

2 The micro-lens array, in conjunction with the first encountered lens, focuses the beam into the end of the optical fiber selected by Bragg Cell 1.

3 The grin lenses are used to collimate the output of the optical fiber before deflection by the next Bragg cell. The purpose of the components used thus far are to make usable, the space-bandwidth product of the Bragg Cell 1 via selection, physical separation, and collimation of the readout beams.

4 Once the desired volume is selected, the desired angle-multiplexed page is selected using the next Bragg cell.

5 Recorded information is extracted from the hologram substrate library by illuminating the desired volume location (via Bragg cell #1) and by adjusting the incident angle (via Bragg cell #2).

6 The reconstructed wave-fronts are inverse Fourier-transformed by the lens and the resulting page of binary information (in the form of presence or absence of light) is then incident on the pads of the CMOS detector IC.

TABLE 3.2 THE WRITE SYSTEM

1 Light from an argon laser (λ=514.5 nm) is split into two paths by beam splitter (BS).

2 One beam is incident on the data mask consisting of an array of windows 40 um wide on 100 um centers.

3 The data mask's information is transformed by the lens to take advantage of the shift invariance of the Fourier-transform: a vital property in the readout system.

4 The Fourier-transform pattern is "low pass filtered" by a hard aperture immediately before reaching the holographic recording medium. This is necessary for a high data storage density.

5 The reference beam is reflected from rotatable mirror one focal length away from the first lens in a telescope.

6 The focal lengths of the telescope lenses can be adjusted to trade off the angle and beam diameter of the light reaching the hologram.

7 A hologram (page) is recorded in the substrate (LiNbO3) and a new data mask is placed in the system. Then the page selection mirror is rotated to a different angle and the process is repeated. After approx. 10 pages have been recorded in this manner, the substrate is translated to expose fresh material and the angular multiplexing is performed again.

Each part of the read system has been designed, assembled, and individually tested for throughput. The results of these individual throughput measurements have been tabulated and are shown at their respective sites along the system in Figure 3.4.

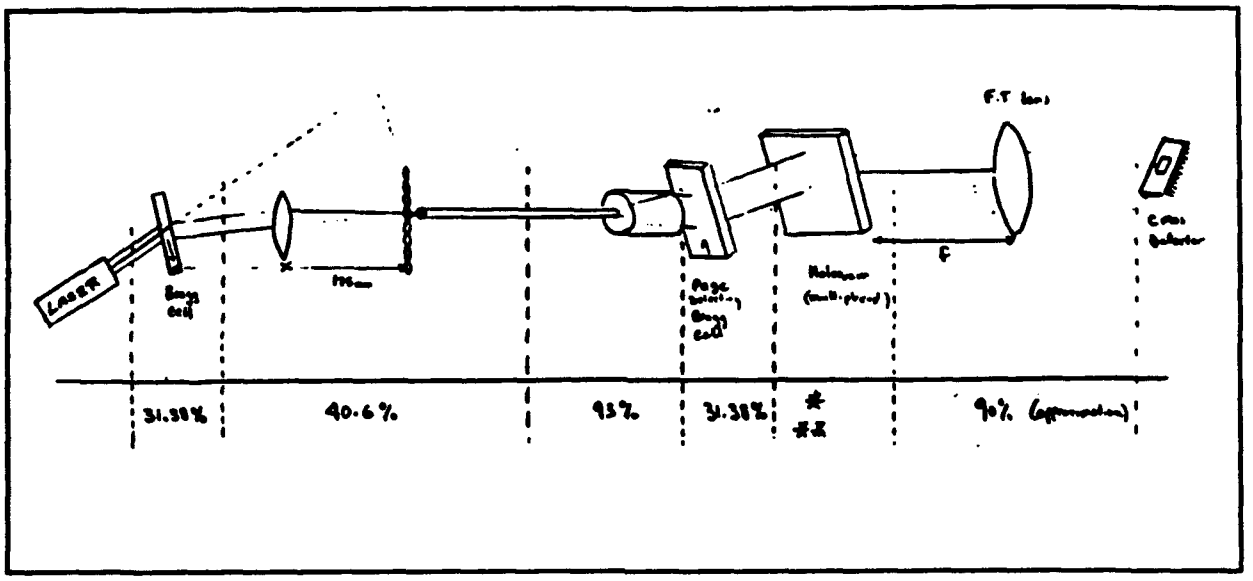

Figure 3.4 Exploded view of the read system showing the transmission efficiency of each of the components. The total measured efficiency is 1.6%.

The hologram "throughput" is dependent upon several factors including the refractive index dynamic range available, the number of holograms multiplexed, and the number of "on" bits in the object. As an example, consider a volume in which we write 10 multiplexed plane-wave holograms. Assume that to conserve the available Δn and to avoid cross talk, each of these has a 10% diffraction efficiency. Now, since the object fill factor ratio is inversely proportional to the square of the object aspect ratio (bit center to center spacing divided by the bit width), for a fully populated mask with 50 micron features on 100 micron centers, only 25% of the available surface area of the object is illuminated, thus the maximum throughput for this pattern would be (10%)(25%) = 2.5%. Notice in Figure 3.4, that the measured throughput for 1 of 5 multiplexed hologram patterns with a 25% fill factor is 1.6%, in reasonable agreement with the estimated value of 2.5%.

Figure 3.5 shows the readout of five multiplexed hologram patterns using the optical fiber - GRIN lens - Bragg cell combination to select the proper angle. The holograms were sequentially written according to an exponential writing schedule to equalize the diffraction efficiencies. A linear detector array was used to measure the bit uniformity within each hologram and each two dimensional object pattern is shown with the one-dimensional scan through it's center generated by the output from the array.

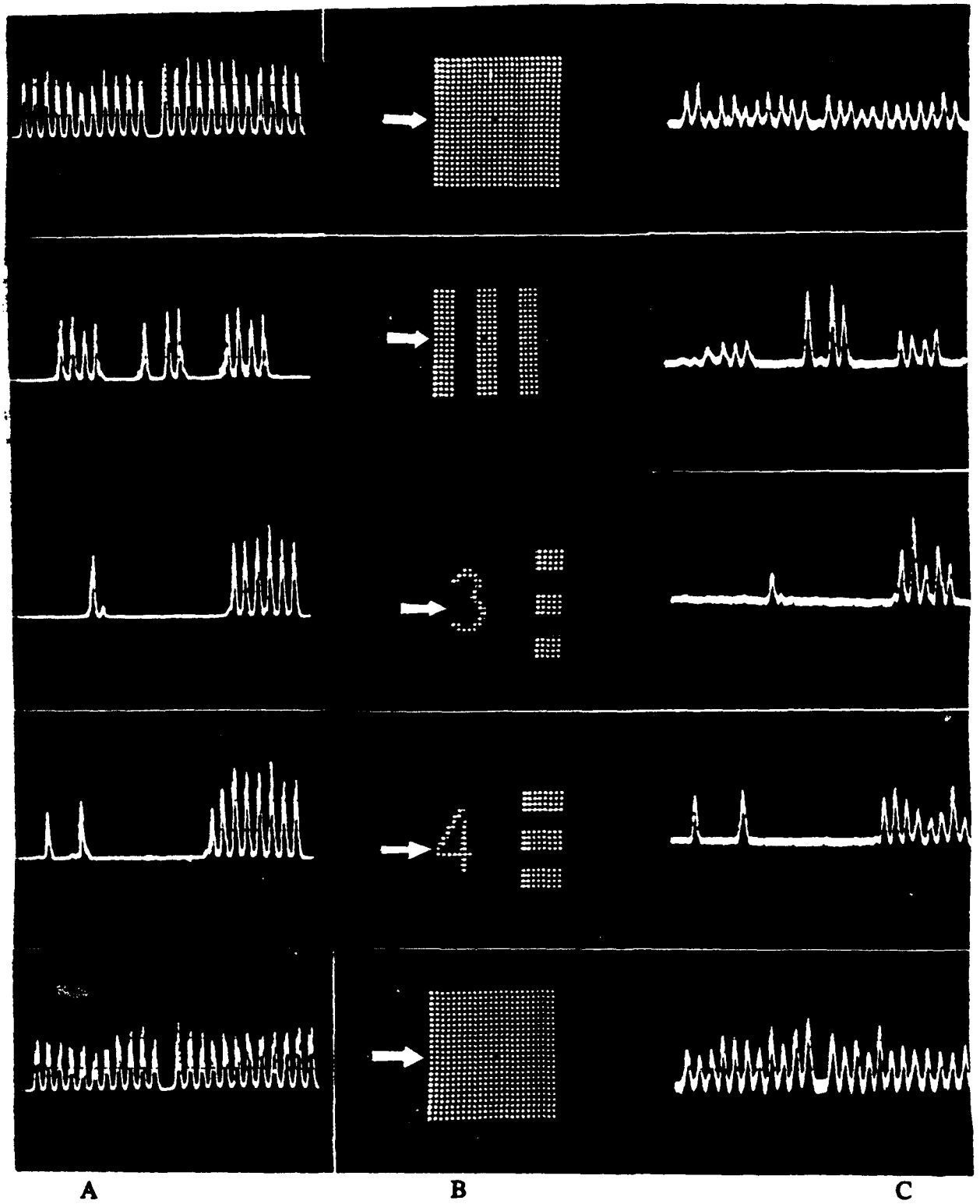

Figure 3.5 B) Photographs of five digital patterns whose Fourier-transform holograms were recorded in a 1-mm thick $LiNbO_3$ crystal in lieu of a suitably thick polymer sample. Linear detector-array scans of the indicated track in A) a real image and in C) the holographic reconstruction of the digital patterns.

4. OPTICAL-ELECTRONIC CMOS CIRCUITS

The system described in this research is designed to transfer data from an optical hologram into a high-speed, integrated electronic chip for direct access by a conventional electronic processing network. Several approaches were considered for implementing the desired functions. The specifics of the circuits are summarized below.

The design, analysis, and fabrication of the electronic RAM array was performed using the 2-micron CMOS process available through MOSIS (MOS implementation service). The electronic chip design for the project was broken down into three major segments: (a) integrated optical detectors in an existing CMOS technology, (b) the design and analysis of an optically-loaded RAM cell array, and (c) an exploration of more advanced applications of the concepts.

In this project, a high-speed integrated CMOS process was chosen for its logic-integration capabilities. Adding the photodetector and associated circuitry to the normal design procedures provides for direct optical-to-electronic interfacing. However, since the fabrication process is optimized for electronic performance, it is not possible to alter the doping profiles to increase the responsivity of the photodiodes. Interest thus revolves around providing a reasonably sensitive detector/circuit which can be directly interfaced to standard logic designs.

4.1 Optical Detectors

Several types of integrated optical detector circuits can be fabricated directly in a bulk CMOS process using the various pn junctions which are intrinsic to the structure. In this research, many types of circuits were studied for their suitability in the memory array. Chapter 3 of the Ph.D. thesis by A. Sayles entitled "Design of Integrated CMOS Circuits for Parallel Detection and Storage of Optical Data" (see Appendix C) provides a thorough discussion of the analysis and modeling of four photodetector circuits. Moreover, the manuscript "Optical Detectors in Bulk CMOS" by Henderson and Uyemura (see Appendix D) compares the most important circuits in terms of optical-electronic performance, chip layout area, and overall output characteristics.

The circuit which was chosen as optimal in both studies is shown in Figure 4-1. It consists of a photodiode operating in the photoconductive mode with a p-channel MOSFET Mp acting as a pull-down device. The operation is straightforward. When light strikes the diode, light current flows to charge the capacitor C_{out}. In this circuit, an n-channel MOSFET has been added to provide for rapid discharge using a clear (CLR) pulse as shown. This circuit provides an excellent trade-off between speed and layout requirements.

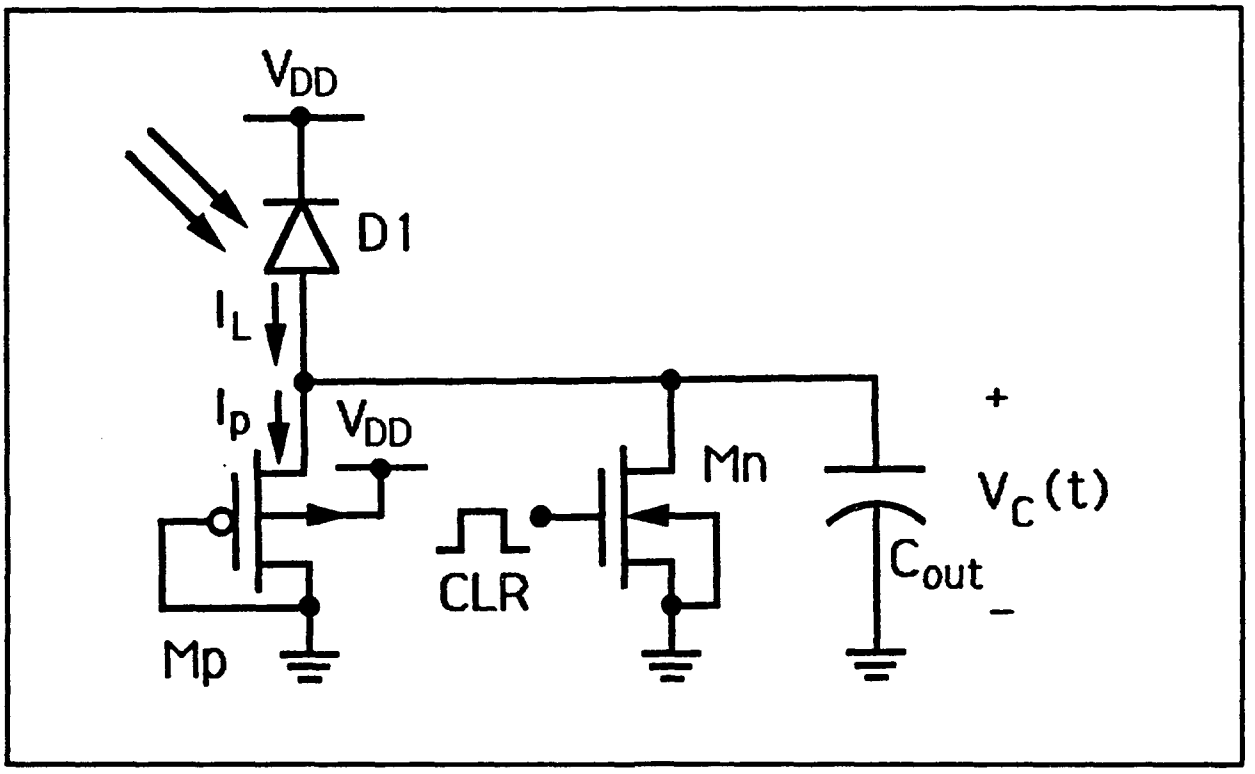

Figure 4.1 A photodiode operating in the photoconductive mode with a p-channel MOSFET Mp acting as a pull-down device.

4.2 RAM Cell Array

The second phase of the electronics design centered around the design, fabrication, and testing of various RAM arrays for use in the optical-to-electronic data transfer system. The most important aspects in this portion of the research were (i) speed of data loading, (ii) cell density, and (iii) interfacing with the optical hologram.

The details of the design have been published in two sources: Appendix E, Sayles and Uyemura, "An Optoelectronic CMOS Memory Circuit for Parallel Detection and Storage of

Optical Data" (in the IEEE Journal of Solid State Circuits), and in Appendix C, the Ph.D. Thesis of A. Sayles. Only a brief summary of this work is presented here.

The primary prototype design was a 4 x 4 array of static RAM cells with optical data loading circuits added. System operation is initiated with an electronic clear pulse which places a logic 0 in each cell. Exposure to the holographic light pattern selectively writes logic 1 states to the proper cells. Both electronic and optical write operations were possible with the circuit. The initial array was made using 100 micron x 100 micron cells; each cell contained a RAM circuit, a 10 μm x 10 μm photodiode, and the associated interface circuitry. Subsequent designs were made down to a 60 μm x 60 μm cell using the MOSIS 2-micron CMOS process; in addition, we investigated a 40 μm x 40 μm cell for use in the MOSIS 1.2-micron CMOS line. Current designs have progressed to a 16 x 16 array, providing 256 individual bits of data. Apparent limitations are due to the CMOS lithography and design rule constraints.

Some iterations were required to obtain a circuit design which was relatively immune to the process variations which were, at times, deviated as much as a 100 percent from nominal design values. However, use of the balanced RAM networks and judicious choice of the transistors in the optical load circuitry allowed us to demonstrate positive results in both the electronic and optical-electronic experiments.

The transient response of the optical-input circuitry could not be measured directly. However, additional test circuits indicate a worst-case loading time of 200 nsec with an input optical power of 3.5 μwatt; this represents the lower detectable power per pixel with the standard MOSIS 2-micron CMOS process. Since, for a given circuit, the switching time is inversely proportional to the incident optical power, an estimate of the RAM writing time for other optical powers can be extrapolated.

4.3 Advanced Applications and Concepts

The third segment of the electronics studies was concerned with the application of the circuit techniques and extending the work to more advanced systems. This work is still in progress, but is described in the manuscript "Integrated PhotoMOSFETs" by Austin and Uyemura (Appendix E), and in the Uyemura and Austin paper "Hybrid optical-electronic

logic gates in complementary metal-oxide semiconductor very-large-scale integration" published in Applied Optics (Appendix F).

The concepts which were developed in this work build on the fact that it is possible to integrate a photodiode directly into p- and n-channel MOSFETs, which expands the integration capabilities of the system. In addition, proper use of the photoMOSFETs allows one to construct hybrid optical-electronic logic gates which accept both optical and electronic input logic states, and provide an electronic result. As discussed in the referenced papers, optical signals can be used to represent either control or data states in standard static CMOS logic circuits.

Dynamic CMOS circuits were chosen for use in the studies because of the speed advantage, and due to the various system design styles which are available for advanced logic applications. With basic dynamic operation, it was possible to develop Boolean logic formation rules for the hybrid logic gates. These can be extended to the more advanced CMOS design styles of domino logic, multiple-output domino logic, and NORA structures.

Many applications can be perceived using this type of hybrid circuit. Systems which require optical-electronic feedback (such as one using an electronically-controlled spatial light modulator) are immediate candidates for the technology. More advanced systems which have been proposed here include hybrid optical-electronic neural networks, optically-controlled microprocessor instruction set design, and electronic parallel processors with optically-reconfigured architectures. Direct interfacing with existing optical computer schemes has also been investigated.

5. MATERIAL STUDIES

5.1 Introduction

The various photosensitive inorganics and organics useful for the holographic memories can be divided into two broad categories, viz., those requiring development and the self-developing type. For those requiring development, the steps of formation of a latent image, transformation into a real image through wet or dry development, and fixing using either wet or dry technique, are involved. In the self-developing type, however, the first two steps are eliminated, and the third step may or may not be required. Under the former type we can enumerate the following classes of materials: photographic emulsion; photoresists; electro-photographic materials; and photoplastics. Among the latter type are: photothermics; photoconductors; magnetooptic; photochromics; photopolymers; photorefractives; and photochemical holes[7].

A satisfactory volume holographic recording material must have the following properties:

- A dynamic range large enough to ensure sufficient modulation
- Environmental stability for long periods
- No distortion
- Low scattering

In addition, the thickness of the material precludes chemical processing. Therefore, thermal or optical processing and fixing is desirable. To overcome the problem of fabricating and processing thick emulsions, several researchers investigated multilayer holograms to produce the effect of a thick material[8,9]. In such hologram successive thin gratings are separated by spacers. Diffraction efficiency depends mainly on the sum of the grating thicknesses, while angular selectivity is governed by the total thickness of the stack. The combination of high diffraction efficiency and tailored selectivity makes multilayers attractive, but more work is needed to assess their potential. Assembly of the layered structure is also a major problem, but this may be overcome.

5.2. DuPont Photopolymer

No real-time recording materials satisfy all of the conditions mentioned above. However, photopolymers are worthy of consideration as volume holographic material because of several attractive advantages[10,11]. These include self-developing, dry processing, good stability, thick emulsion, high sensitivity, large diffraction efficiency, high resolution, and nonvolatile storage.

We investigated the DuPont photopolymer (D.P.P.) which consists of a polymeric binder, photoinitiator system, sensitizing dye(s), polymerizable monomers basically; occasionally, other ingredients such as plasticizer, surfactant, and solvent(s)[12,13,14]. The HRF-150-38 transmission type DuPont photopolymer film is a 38-micron-thick emulsion that is sandwiched between a 50-micron Mylar base and a thinner Mylar coversheet. In general, recording mechanism is a three step process. First, an initial exposure records the interference pattern. This initial exposure polymerizes part of the monomer, with the amount of polymerization being a function of the integrated intensity of the illumination. Monomer concentration gradients, caused by variations in the amount of polymerization, then give rise to the diffusion of the somewhat small monomer molecules from regions of higher concentration to regions of lower concentration. Second, a uniform postexposure is required for dye bleach and complete polymerization. This can be done with one of the two interfering beams or with a fluorescent or U.V. light. Third, an optical annealing process enhances index modulation in the already formed hologram.

5.2.1 Plane Wave Studies of Fundamental Characteristics

Holograms were written using 1 milliwatt 1-cm-diameter, 514.5-nm beams derived from an argon-ion laser. A conventional hologram-writing arrangement was used in which the optical system for recording the grating structure provided uniform, collimated beams symmetrically disposed about the normal to the material surface. The incidence angles of the two beams outside the material are 24 degrees each. During exposure the emerging hologram is probed with a 632.8 nm He-Ne laser beam which, because of the film's very poor red sensitivity, does not perturb the system. The probe beam of the is detected by photodetector and its intensity is plotted on a chart recorder.

Under these conditions, a one-layer photopolymer film has a characteristic curve which saturates rather than exhibiting a maximum. A two-layer film was prepared by removing the Mylar cover sheets from two of the 38-micron-thick photopolymer film which were then laminated face to face and attached to a glass substrate. As shown in Figure 5-1, the diffracted 632.8 nm power exhibits a true maximum because, unlike the prior case, there is now a sufficient product of index modulation with hologram thickness to allow the diffraction efficiency to pass the first maximum of the sin^2 curve.

The maximum index of refraction modulation calculated from Kogelnik's coupled wave theory is 0.0076. The bulk refractive index of the medium is n_o = 1.49-1.51. It is difficult to further increase the film thickness by multiple laminations because the base Mylar cannot be removed before polymerization is completed.

Angular selectivity measurements were also carried out. The results agreed with theoretical expectations. The angular full width at half maximum for the single emulsion layer is 1.2 degrees.

Appendix G contains a detailed account of this work.

5.2.2. Dynamic Properties and Shrinkage

A number of measurements were made in an attempt to elucidate the details of the recording process in the DuPont material. These are discussed in Appendix H. The role of physical parameters such as, exposure, exposure time, processing, thickness, storage, were considered. After optical fixing, the Dupont materials were found to be stable against environmental factors such as such as humidity, temperature and ambient light.

The only significant negative aspect of the DuPont materials is the fact that there is a noticeable shrinkage of the material, most of which occurs during the fixing process when the all of the residual monomer is polymerized. The DuPont photopolymer was chosen with the expectation that this effect would be quite small, because there is no wet processing as in photographic emulsions or dichromated gelatin. Unfortunately, the shrinkage exceeds 2%. The effects are demonstrated quite clearly in the experimental results shown in Figure 5-2 in which the Bragg-angle deviation due to shrinkage is plotted against the as the slant angle of

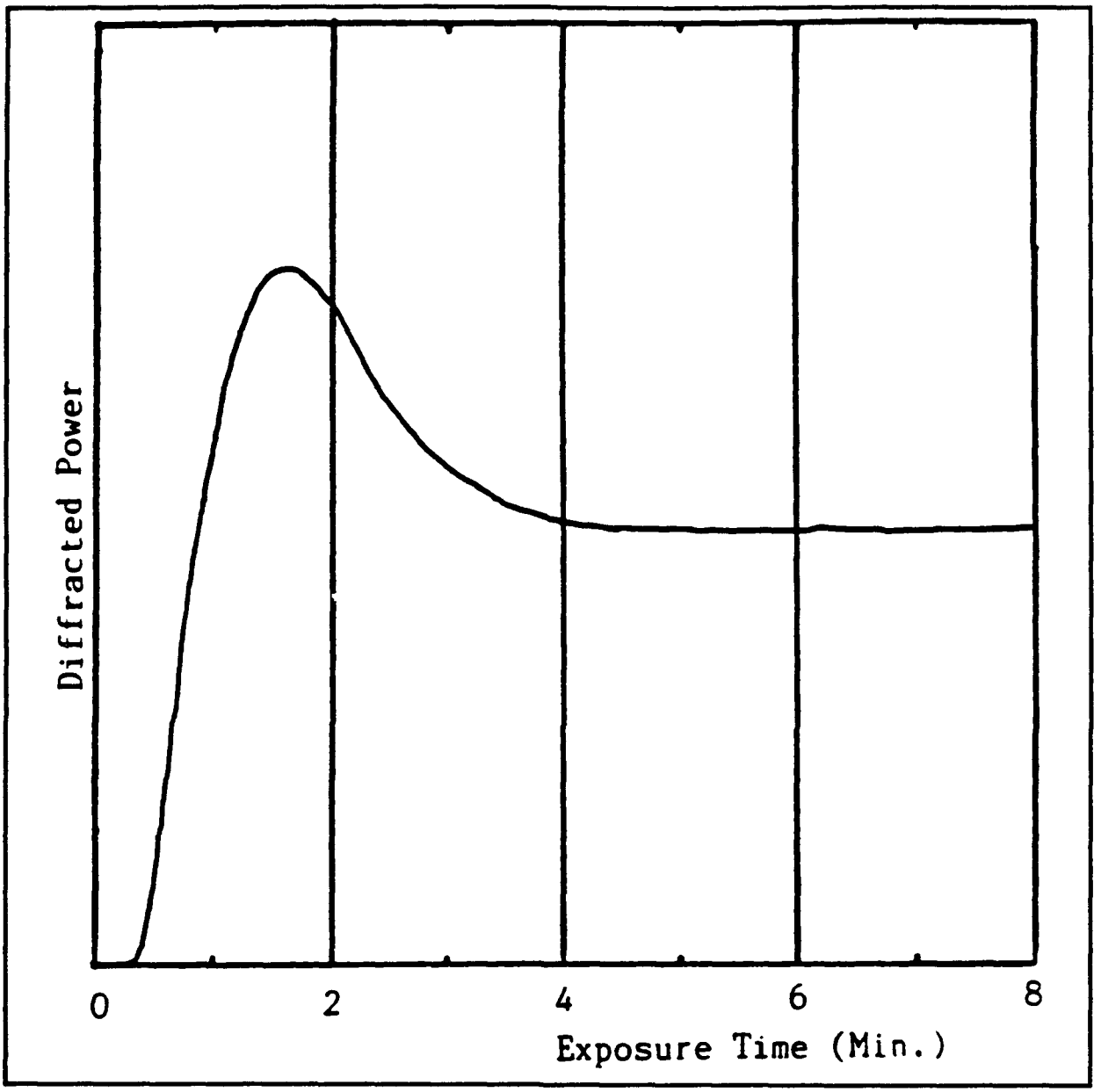

Figure 5.1 Diffracted power versus exposure time for a plane-wave hologram in a 76-μm-thick emulsion with 1.27-mW/cm^2 beam intensities.

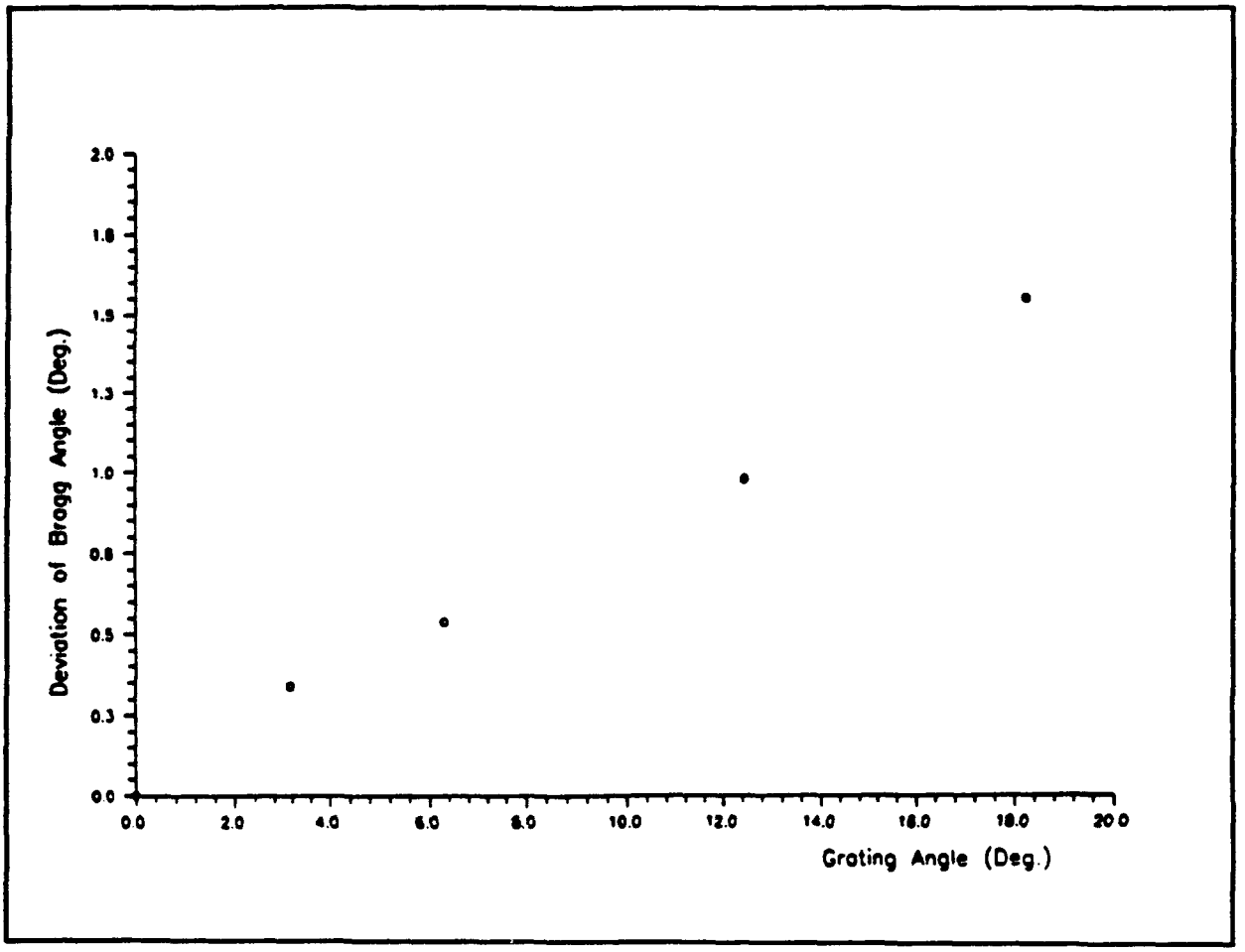

Figure 5.2 Measured deviation of the reconstruction Bragg angle versus grating slant angle. From these the shrinkage is estimated to be 2.5%.

the grating. As expected, the deviation goes to zero for a symmetric grating, that is, a grating with zero slant angle. Unfortunately, other considerations, to be discussed below, make it difficult to use the symmetric grating geometry in the POHM architecture.

5.2.3 Shrinkage Prevention or Reduction in Photopolymers

An attempt was made to stabilize the geometry of the photopolymer by infiltrating a solution of the photopolymer into a porus glass matrix. This solution consists of monomer, binder, initiator, plasticizers, sensitizer and so on, into which the porous glass is dipped. Inspect the samples revealed two major problems: First, the solution can not penetrate into the pores of glass because this solution is approximately 50% solids in 2 - butanone/toluene solvent system. The viscosity, which is ~ 15,000 cps at 20°C for shear rates of 0.4 - 2 S^{-1}, is

too high . Second, although the porous glass is transparent before and during dipping in the solution, after its surface touches the air, it develops a milky appearance. We need the photopolymer solution without the solid components, for example, plasticizer and polymeric binder which work for dimensional stability of dry film. However, we were unable to obtain these special materials.

5.3 Summary and Recommendation

In addition to the DuPont photopolymer, silver halide photographic material (KODAK 649-F and KODAK 120), dichromated gelatin (D.C.G.), , and dichromated polyvinyl alcohol (DC-PVA) films were investigated as POHM recording materials.

Of these, the photopolymer film is recommended for the purpose of making holographic memories with large information storage capacity because of the following advantageous properties: self-developing, dry, rapid processing, reasonably high sensitivity, adequate Δn, high resolution, and nonvolatile storage. However, before this film can be used in a practical systems, several problems must be solved. First, it is necessary to develop a for increasing thickness of emulsion to 1 mm without losing good its optical characteristics. Second, reducing the structural distortion (shrinkage/swelling) by using a porous glass technique or new chemical components. We believe that both of these problems could be solved with the active participation of the manufacturer of the material.

Because of the problems in obtaining perfect materials, a number of optical techniques for reducing, or for better understanding the material requirements were investigated. These are described in the following Section.

6. OPTICAL COMPENSATION FOR MATERIAL LIMITATIONS

6.1 The Use of Phase Plates to Extend Dynamic Range

All optical recording materials have a finite dynamic range. In recording phase holograms, the appropriate measure of dynamic range is derived from the expression for the diffraction efficiency,

$$\eta = \sin^2\left[\frac{\pi \delta n t}{\lambda_o \cos\Theta_B}\right] \tag{4}$$

where δn is the index modulation and t is the material thickness. We have seen that, to obtain sufficient angular resolution, we require $t \geq 1$ mm. For a Bragg angle of 20°, and a wavelength of 514 nm, 100% diffraction efficiency is achieved when

$$\delta n t = \frac{\lambda \cos\Theta_b}{2} = 2.4 \times 10^{-4}\, mm. \tag{5}$$

Therefore, for a 1-mm thick material we require a δn of 2.4×10^{-4}. It is more realistic, and less likely to produce crosstalk if we aim for a 20% diffraction efficiency. In this case $\delta nt = .7 \times 10^{-4}$. The measured value of the available index modulation in the DuPont photopolymer is $\Delta n = 76 \times 10^{-4}$, so it would seem that there is sufficient index modulation available to produce over 100 holograms.

The theory upon which the above conclusion is based assumes that the holograms written by interfering plane waves which produce a uniform sinusoidal grating. However, the Fourier transform of a periodic object such as a binary page mask has a very uneven distribution of optical energy. The irradiance in the rear focal plane of a lens of focal length f, due to single square aperture of width w located in the front focal plane, is a $sinc^2$ function with a peak intensity proportional to d_4. The Fourier transform of an N × N array of such apertures is a series of spikes within a $sinc^2$ envelope. However the central spike has an intensity proportional to N^4d^4. So, for example, for a 32 × 32 array the recording material is subjected to an intensity spike some three orders of magnitude higher than for a single aperture. The result is that the material may experience local saturation even for a single

exposure. This can result in an aberrated reconstruction of the hologram in the case of a single image and possible crosstalk in the case of multiple holograms stored in the same volume.

The problem of nonuniform irradiance can be alleviated, to a large extent, by the incorporation of phase shifts between the individual apertures which represent the data bits. The result, as shown in the experimental profiles in Figure 6 of Appendix I is that the energy is spread over the entire $sinc^2$ curve rather than being concentrated in a few spikes. Although is not evident in the photographs, the total energy arriving at the detector plane is the same in both cases.

Appendix I, is a report on a six-month project related to the current program and to a Georgia-Tech-supported binary optics project. It discusses both the theory of the use of phase diffusers and the effects of fabrication tolerances on their operation. In spite of the many papers which have been published on the use of random phase plates to perform phase averaging, it is concluded that, because of their relative tolerance to fabrication errors, it is beneficial to use a deterministic phase grating to perform the phase averaging operation.

6.2 Minimizing the Effects of Shrinkage on the Reconstructed Image

Because of the many favorable characteristics of polymeric recording materials, it is essential that the effects of shrinkage, their most undesirable characteristic, be well understood. The simplest way to negate the shrinkage effects is to write all holograms as symmetric holograms, that is with the reference beams and the signal beam making equal angles to the material normal. In this configuration, all the fringes are normal to the surface and fringe rotation, which is the most detrimental effect of shrinkage, is eliminated. This complicates the writing process since the reference beam angle must change without changing the location of the reconstructed image. A reasonable solution to this problem was found for angle multiplexing a number of holograms in a single volume. However, the issue is moot because of a more fundamental problem which arises when a large number of hologram volumes are contained on a single memory plane.

The more fundamental problem arises from the fact that, in order to write a symmetric hologram, the recording plane must be at an angle to the signal beam. This, in turn means that the recording material does not lie in the front focal plane of the retransform lens, but in

fact, lies at an angle to this plane. It is therefore not possible to reconstruct an extended array of Fourier-transform holograms without severe aberration. For this reason, the effects of shrinkage on holograms written with the signal beam normal to the recording plane were investigated in some detail.

The results of the shrinkage investigations are contained in Appendix J, a manuscript which has been submitted to Applied Optics. The work, which is based on the fringe-rotation model, indicate that shrinkage of the recording material results in a reduction of diffraction efficiency, broadening of the image features and a reduction in signal-to-noise ratio. However, there is no shift in the image position. Furthermore, the effects of shrinkage can be somewhat mitigated by the proper selection of recording geometry.

7. CONCLUSIONS AND POTENTIAL APPLICATIONS

7.1 Conclusions

The ability to fabricate CMOS arrays with sensitive optical detectors in each cell and the ability to address an angle-multiplexed hologram array using an optical system composed of two Bragg Cells coupled by a fiber array has been demonstrated. The optical efficiency of address system is dominated by the TeO_2 Bragg-cell efficiencies of 31% If we replace these with 90% efficient $LiNbO_3$ cells, then the efficiency of the hologram addressing system would be 30%. From the hologram reconstruction efficiency data presented in Section 3 and the CMOS sensitivity data presented in Section 4, we conclude that, if the duration for which the CMOS is exposed to a data pattern is 1 μsec, then with a 1-Watt laser there is enough optical energy for the CMOS to detect over 6800 bits. It would therefore seem reasonable to predict that, using a 2.5 Watt laser, a 128 × 128-bit system could be successfully constructed, predicated on the availability of 1-mm thick photopolymer sheets. Using 5-mm wide TeO_2 Bragg cells, the access time per page will be limited by the acoustic transit time to about 8 μsec. Use of a $LiNbO_3$ cell would improve this figure by a factor of 10. Allowing 0.2 μsec for addressing, we could therefore anticipate a data rate of

$$128^2 \text{ bits/page} \times 5 \times 10^5 \text{ pages/sec} = 8 \times 10^9 \text{ bits/sec.}$$

The use of the fiber cable between the position and angle- selecting Bragg cells will allow this system to be housed in on two standard 19" chassis. The fiber cable can further provide the flexibility to address more than one CMOS chip with the same holographic ROM.

7.2 Potential Applications

The system described here is designed for parallel data transfer from an optical ROM into an arbitrary electronic processing component. The CMOS RAM array was chosen as the starting vehicle due to the immediate application in accessing optical data by an electronic system. However, the idea can be extended far beyond the original proposal due to the generality of the concepts involved. Some of the most promising systems for future

application are described below. Details, where available, can be found in the papers provided in the Appendices.

7.2.1 Hybrid Optical-Electronic Logic Gates

In this type of system, the optical data can be directly combined with electronic inputs for the purpose of performing Boolean logic. This provides for immediate processing of optical data for direct access by electronic means.

7.2.2 Optical Control of Electronic Data Paths

The concepts have been applied to the case where electronic switching networks can be directly controlled by an optical input matrix. This allows for direct reconfiguration of an arbitrary classical network.

7.2.3 Optically-Reconfigured Microprocessor

In this VLSI design, the instruction set of the microprocessor is under direct control of the optical data matrix. The logic is designed using photo-MOSFETs so that changing the holographic image induces a change in the instruction set of the processor.

7.2.4 Optically-Configured Parallel-Processing Architectures

Combining the ability to optically alter both the data paths and the instruction set of a microprocessor gives rise to a new class of parallel-processing schemes. Both SIMD and MIMD architectures are possible using the basic ideas. Other schemes, such as optically-controlled hypercubes, can also be envisioned.

LIST OF ALL PUBLICATIONS AND TECHNICAL REPORTS

1. John T. Gallo, "Design of a Holographic Read-Only-Memory for Parallel Data Transfer to Integrated CMOS Circuits," Ph.D. Thesis, Georgia Institute of Technology, August 1991.
2. J. T. Gallo, M. L. Jones, and C. M. Verber, "Computer Modeling of the Effects of Apertures in the Fourier-Transform Plane of the Fourier-Transform Imaging Systems," manuscript submitted for publication, July 1992.
3. Andre Harding Sayles, "Design of Integrated CMOS Circuits for Parallel Detection and Storage of Optical Data," Ph.D. Thesis, Georgia Institute of Technology, August 1990.
4. Karen E. Henderson and John P. Uyemura, "Optical Detector Circuits in Bulk CMOS," manuscript submitted for publication.
5. Blanca L. Austin and John P. Uyemura, "Integrated PhotoMOSFETs," manuscript submitted for publication.
6. John P. Uyemura and Blanka L. Austin, "Hybrid Optical-Electronic Logic Gates in Complementary Metal-Oxide Semiconductor Very-Large-Scale Integration," Applied Optics, vol. 31, no. 11, pp. 1774-1782, April 10, 1992.
7. Uh-Sock Rhee, H. John Caulfield, Joseph Shamir, Chandra S. Vikram, and Mir M. Mirsalehi, "Characteristics of DuPont Photopolymer for Angularly Multiplexing Page-Oriented Holographic Memories (POHMs)," manuscript submitted for publication.
8. Uh-Sock Rhee, H. John Caulfield, Chandra S. Vikram, and Joseph Shamir, "Dynamics of Hologram Recording in DuPont Photopolymer (D.P.P.)," manuscript submitted for publication.
9. Menelaos Poutous, "Phase Diffusers for Digital Holography Using Diffractive Optical Elements," Special Problems in Electrical Engineering Course Term Paper for EE-8500, Spring 1992.
10. J. T. Gallo and C. M. Verber, "Simulation of the Effects of Material Shrinkage on Fourier-Transform Holograms," manuscript submitted for publication, June 1992.
11. Uh-Sock Rhee and H. J. Caulfield, "Side-Lobe Suppression in Angularly Multiplexed Holograms," manuscript submitted for publication.

LIST OF ALL PARTICIPATING SCIENTIFIC PERSONNEL

Blanca L. Austin

H. John Caulfield

John T. Gallo: Earned Ph.D. in August 1991

Mark. L. Jones

Mir M. Mirsalehi

Uh-Sock Rhee

Andre Harding Sayles: Earned Ph.D. in August 1990

John P. Uyemura

Carl. M. Verber

Chandra S. Vikram

REFERENCES

1. B. M. Monroe, W.K. Smothers, R. R. Krebs and D. J. Mickish, "Holographic Photopolymers" SPSE 40th Annual Conference and Symposium on Hybrid Imaging Systems, May, 1987, Rochester, NY.

2. L. d'Auria, J. P. Huignard, C. Slezak, and E. Spitz, Appl. Opt. **13**, 808-818 (1974); H. Kiemle, Appl. Opt **13**, 803-807 (1974); Richard G. Zech, "Data Storage in Volume Holograms," Ph.D. Dissertation, Univ. of Michigan, 1974.

3. F. M. Smits and L. E. Gallagher, Bell Syst. Tech J. **46**, 1267-1278 (1967).

4. Richard Gerald Zech, "Data Storage in Volume Holograms," Ph.D. Thesis, U. of Michigan, 1974.

5. Thomas K. Gaylord, "Digital Data Storage," in *Handbook of Optical Holography*, H. J. Caulfield, ed., Academic Press 1979.

6. Awing Gi Pack, John R. Wullert, II, M. Jain, A. Von Lehmen, A. Scherer, J. Harbison, L.T. Florez, H. J. Yoo, R. Martin, J. L. Jewell and Y. H. Lee, Optics Lett. **15**, 341-343 (1990).

7. W. E. Moerner and M. D. Levenson, "Can single-photon processes provide useful materials for frequency-domain optical storage?," J. Opt. Soc. Amer., B2, 915-924 (1985).

8. B. Y. Zel'dovich and T. V. Yakovleva, "Theory of a two-layer hologram," Sov. J. Quantum Electron. 14(3), 323-328 (1984).

9. A. P. Yakimovich, "Multilayer three-dimensional holographic gratings," Opt. Spectrosc. 49(1), 85-88 (1980).

10. W. J. Tomlinson, E. A. Chandross, H. P. Weber, and G. D. Aumiller, "Multicomponent photopolymer systems for volume phase holograms and grating devices," Appl. Opt. 15, 534-541 (1976).

11. S. Calixto, "Dry polymer for holographic recording, " Appl. Opt. 26, 3904-3910 (1987).

12. A. M. Weber, W. K. Smothers, T. J. Trout and D. J. Michish, "Hologram recording in DuPont's new photopolymer materials," in Practical Holography IV, Proc. SPIE 1212, 30-39 (1990).

13. W. K. Smothers, B. M. Monroe, A. M. Weber and D. E. Keys, "Photopolymers for holography," in Practical Holography IV, Proc. SPIE 1212, 20-29 (1990).

14. W. J. Gambogi, W. A. Gerstadt, S. R. Mackara, and A. M. Weber, "Holographic transmission elements using improved photopolymer films," in Computer and Optically Generated Holographic Optics, Proc. SPIE 1555, 256-266 (1991).